Applied Physics B (2021) 127:46
https://doi.org/10.1007/s00340-021-07588-8

**Applied Physics B**
**Lasers and Optics**


# Comparative investigation of lasing and amplification performance in cryogenic Yb:YLF systems

**Umit Demirbas[1,2] · Martin Kellert[1] · Jelto Thesinga[1] · Yi Hua[1] · Simon Reuter[1] · Franz X. Kärtner[1,3,4] · Mikhail Pergament[1]**

Received: 17 January 2021 / Accepted: 6 February 2021 / Published online: 1 March 2021


**Abstract**
We present detailed experimental results with cryogenic Yb:YLF gain media in rod-geometry. We have comparatively investigated continuous-wave (cw) lasing and regenerative amplification performance under different experimental conditions. In the cw lasing experiments effect of crystal doping, cw laser cavity geometry and pump wavelength on lasing performance were explored. Regenerative amplification behavior was analyzed and the role of depolarization losses on performance was investigated. A recently developed temperature estimation method was also employed for the first time in estimating average crystal temperature under lasing conditions. It is shown that the thermal lens induced by transverse temperature gradients is the main limiting factor and strategies for future improvements are discussed. To the best of our knowledge, the achieved results in this study (375 W in cw, and 90 W in regenerative amplification) are the highest average powers ever obtained from this system via employing the broadband E//a axis.

## 1 Introduction

Yb-doped solid-state laser gain media possess a simple energy level structure that enables low-quantum-defect pumping with high-power laser diodes [1–5]. Moreover, they are mostly immune to undesired processes such as excited-state absorption, cross-relaxation, up-conversion or temperature quenching of fluorescence lifetime. The ideal host for Yb-ions should not only allow for adequately high gain, i.e. enable sufficient Yb-doping with minimal side effects, but it should also combine a broad emission bandwidth with thermo-mechanical strength to assist efficient high-power laser/amplifier operation. Among all the candidates, Yb:YAG has been the most widely studied member. It is shown that, when seeded by optimized broadband sources, Yb:YAG systems have the capacity to support 0.5–2 ps pulse widths at 100 W to kW average power levels [6–9]. Unfortunately, in terms of pulse width, this performance is at the edge for several applications [10] and the search for alternative thermo-mechanically strong host materials with broader bandwidth has been ongoing [11–14]. It is clear that other approaches such as nonlinear spectral broadening for pulse shortening could also benefit from shorter seed pulses [15].

In recent years, we have focused our attention on the YLF ($LiYF_4$) host. In comparison with YAG (865 $cm^{-1}$), YLF has a lower maximum phonon energy (460 $cm^{-1}$), which increases the radiative transfer probability of the active ions [16, 17]. The lower refractive index of YLF (~ 1.45) minimizes radiation trapping effects due to total internal reflection from crystal surfaces [18] and its lower nonlinear refractive index ($1.5 \times 10^{-16}$ $cm^2/W$ [19]) reduces undesired side effects observed in high-power mode-locking [20, 21] or high-energy amplification.

Lasing in Yb:YLF has been first demonstrated as early as 2001 [22]. The room-temperature (RT) bandwidth of Yb:YLF is broad enough (996–1076 nm [23]) to support sub-100-fs pulses [24]. However, at RT, the materials' thermomechanical properties limit the achievable power levels to around 1 W in rod [25], 3 W in waveguide [26] and to

✉ Umit Demirbas
uemit.demirbas@cfel.de

1 Center for Free-Electron Laser Science, Deutsches Elektronen-Synchrotron DESY, Notkestraße 85, 22607 Hamburg, Germany

2 Laser Technology Laboratory, Department of Electrical and Electronics Engineering, Antalya Bilim University, Antalya, Turkey

3 Physics Department, University of Hamburg, Luruper Chaussee 149, 22761 Hamburg, Germany

4 The Hamburg Centre for Ultrafast Imaging, Luruper Chaussee 149, 22761 Hamburg, Germany

6 W [27] in thin-disk geometry. As a solution, Yb:YLF gain media are operated at cryogenic temperatures, which improves their thermomechanical properties [28–31]. Interestingly, the emission spectrum of Yb:YLF crystals stays relatively broad even at cryogenic temperatures (FWHM: ~ 10 nm in E//a axis) [22, 29, 32], and can potentially enable generation/amplification of sub-250-fs level pulses [28]. By employing cryogenic Yb:YLF crystals in rod-geometry, cw power above 300 W [33, 34], Q-switched power of 150 W [35], amplifiers with 100 W average power [36, 37], and mode-locked pulses with 28 W average power [38] were already achieved.

In this work, we investigate limits to further power scaling in cryogenic Yb:YLF systems in rod geometry. For that purpose, we use for the first time a new method to measure the temperature of Yb:YLF crystals under thermal load in lasing condition. Detailed comparative cw lasing experiments are performed and the effect of Yb-doping, pump wavelength and cavity geometry on laser performance are analyzed. A regenerative amplifier cavity was built to pinpoint the limitations of the rod geometry in amplification. Record power levels are achieved in both cw and regenerative amplification experiments for the broadband E//a axis employed in this work. Limitations of thermal lensing and depolarization loss on laser and amplifier performance have been clearly shown, and paths for possible improvements are further discussed.

The paper is organized as follows: Sect. 2 introduces the experimental setups considered. In Sect. 3, we present the cw and regenerative amplification results with accompanying temperature measurements and in Sect. 4, we conclude with a brief summary and discussion.

## 2 Experimental setup

Figure 1 shows the schematic layouts of the laser and amplifier setups we have used in this study. Two different fiber-coupled pump diode modules were tested: (a) a 2 kW system at 960 nm and (b) a 3 kW system at 940 nm. Pumping at 940 nm is interesting because this pump wavelength is often available from pumping Yb:YAG laser systems. At cryogenic temperatures Yb:YLF pumped with E//c axis shows only little absorption around 940 nm, but the E//a axis possesses a broad absorption band covering the 930–950 nm region, with sub-peaks centered around 934 nm and 948 nm (Fig. 2a) [32]. A better option for Yb:YLF is of course the 960 nm absorption peak with a FWHM of around 2 nm: this band is stronger, is available for both polarizations, and enables pumping with a lower quantum defect (Fig. 2c). Assuming lasing at the 1018 nm peak of the E//a axis, the quantum defect under 960 nm pumping is only 5.7% (versus 7.7% for 940 nm pumping).

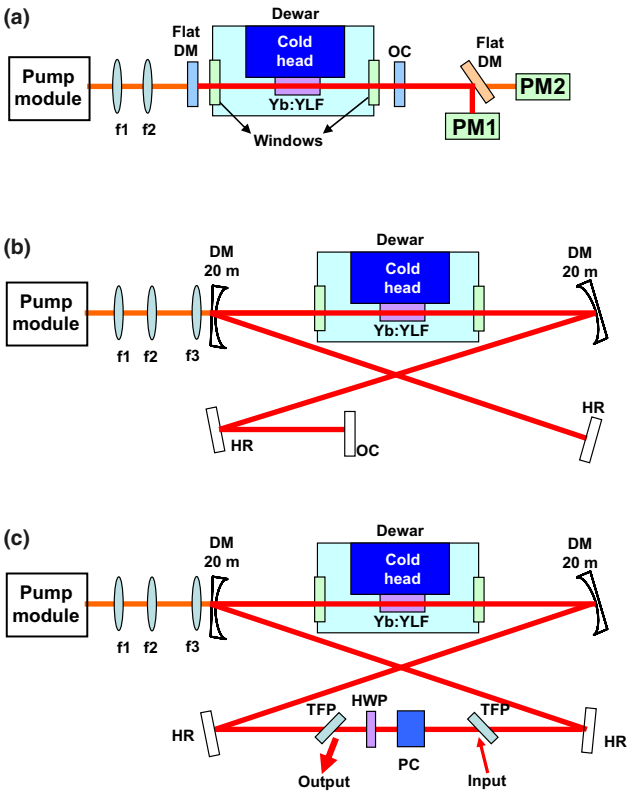


**Fig. 1** Schematic of the Yb:YLF laser used for **a** short-cavity, **b** long-cavity cw laser experiments. Short cavity: flat–flat configuration, long-cavity: x-shaped standing wave cavity with two curved dichroic mirrors. **c** Schematic of the Yb:YLF regenerative amplifier. f1-f3: lenses for pump coupling, DM: dichroic mirror, HR: cavity high reflector, PM1-2: power-meters, OC: output coupler, TFP: thin-film polarizer, PC: pockell-cell, HWP: half-wave plate

In the experiments, a 600 µm core diameter fiber with a numerical aperture (NA) of 0.22 was used to transfer the pump beam from the pump modules (full divergence angle: 25.2°, $M^2$: ~ 220) to the laser crystal. The pump output from the fiber tip is collimated with 72 mm focal length lenses (f1), and focused to a pump diameter of 2.08 mm using lenses with 250 mm focal length (f2). Other pump spot diameters in the 1.5–2.5 mm range were also investigated, but the 2.1 mm spot size was found to be the optimum for the crystals and pump sources used in this study (the root-mean square value of the beam diameter along the crystal length is minimized for this spot size). A discussion of variation of pump beam profile along the crystal length and variation of cw laser performance with pump spot size can be found in [34].

In cw laser experiments, two different cavities have been investigated. In the first case (Fig. 1a), a simple compact flat–flat cavity was employed which consisted of a flat dichroic mirror (DM) and a flat output coupler with a separation of around 28 cm (named as short cavity). The DM had a reflectivity higher than 99.9% in the 990–1040 nm

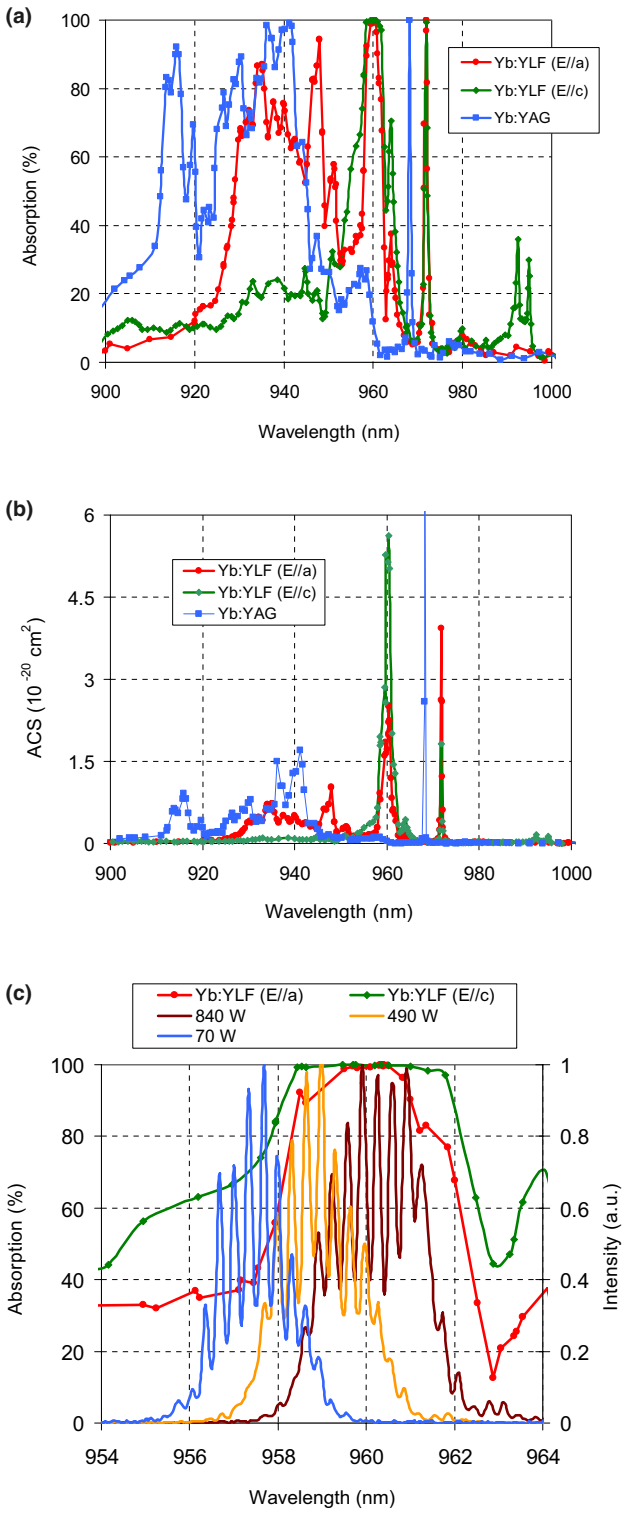


**Fig. 2** **a** Measured small-signal absorption of 2 cm long 1% Yb-doped YLF and YAG crystals at 78 K. Corresponding calculated absorption cross section (ACS) curves are shown in **b**. For Yb:YLF, absorption spectra are shown for both axes. The data are taken using a broadly tunable continuous-wave Cr:LiSAF laser [32]. **c** Measured optical spectra of the 2 kW 960 nm diode at pump power levels of 70 W, 490 W and 840 W, along with the measured small-signal absorption of 1% Yb-doped 2 cm long Yb:YLF. The pump spectral data are taken at a diode cooling water temperature of 30 °C. The central wavelength of the diode could be tuned with temperature with a slope of around 0.35 nm per °C to match the absorption profile of Yb:YLF

range, and a transmission > 95% for the pump wavelengths. In the experiments, output couplers with transmissions of 10%, 20%, 25% and 40% were investigated, and among these the optimum performance was obtained with 25% coupling; therefore, results will only be presented for 25% output coupling.

Two different Yb:YLF laser gain elements were tested with Yb-doping levels of 0.5% and 1%. Both crystals were 20 mm long (with 10 mm × 15 mm cross section), and contained 3-mm-long un-doped end caps diffusion bonded to both ends of the crystals. The crystals were antireflection coated with a simple few-layer coating that is effective both at the pump and laser wavelengths. The crystals were c-cut, and the E//a axis was used for lasing experiments. However, the c-axis of the crystals were oriented $10 \pm 1°$ away from the direction of propagation to create some natural birefringence (a sketch of crystal orientation is available in [37]). The crystals were indium soldered from the top side to a cold head, which was cooled by boiling liquid nitrogen. Antireflection coated windows on each side of the dewar served as entrance and exit ports for the pump and laser beams.

The cw laser performance of the crystals was also tested in a longer standing wave cavity, consisting of two 20 m radius of curvature curved dichroic mirrors, a flat high reflector and a flat output coupler (Fig. 1b). For this cavity, due to the small working-range of the f1-f2 telescope, another 150 mm focal length lens (f3) was used in 2f–2f geometry to re-image the pump beam inside the gain media. The distance between the curved mirrors was around 70 cm in length, and short and long arm lengths were 70 cm and 85 cm, respectively. The cold cavity had a calculated beam diameter of 2.1 mm at the center of the Yb:YLF crystal.

For the regenerative amplification experiments, the standing wave cavity above was converted into a bow-tie type regenerative ring cavity [36]. A half-wave plate (HWP), a Pockell cell (PC) and two thin-film polarizers (TFPs) were used for seeding the amplifier. The regenerative amplifier cavity had a total cavity length of around 3 m, and the cold cavity provided a beam diameter of around 2.25 mm and 2.15 mm at the center of the Yb:YLF crystal and on the PC, respectively. The system is seeded by stretched (~ 1.6 ns) pulses with 20 nJ energy from a fiber front-end, and the details of the seed source can be found in [39]. The seed spectrum was centered around 1019.5 nm and had a FWHM of 2.2 nm. The regenerative amplification is operated at 10 kHz repetition rate, and the system is pulse-pumped at 50% duty cycle using 50 µs long pulses.

The temperature of the crystal was determined by observing the temperature variation of the emission in E//c axis. The ratio of the emission intensity around the 993.5 nm dip to the emission intensity around the 995 nm peak was used for the temperature estimation. This simple technique provides temperature estimation capability with a ± 5 K error bar. The experimental details on this measurement technique can be found in [40].

## 3 Experimental results and discussion

### 3.1 Short-cavity cw lasing results

As a starting point, Fig. 3a shows the measured cw lasing efficiency of the cryogenic Yb:YLF laser using 25% output coupling in the short flat–flat cavity. The measured average temperature of the Yb:YLF crystal under thermal load is also shown in Fig. 3 (temperature data are denoted by open markers in the graph). Two different pump wavelengths are used in the experiment: (a) 940 nm and (b) 960 nm. As we can see from Fig. 3, despite the small difference in quantum defect (5.7% versus 7.7%), there is a clear advantage of using the 960 nm pump. With the 960 nm diode, a record cw output power up to 375 W was achieved at an absorbed pump power of 710 W (incident power: 795 W, absorption: ~ 89.3%). The lasing threshold was around 85 W. The slope efficiency with respect to absorbed pump power was initially around 73%, and gradually decreased to 40% for an absorbed pump power above 600 W (a fit to the whole data set results in a slope efficiency of 61.5%). The overall optical to optical conversion efficiency of the system is around 47% (375 W/795 W).

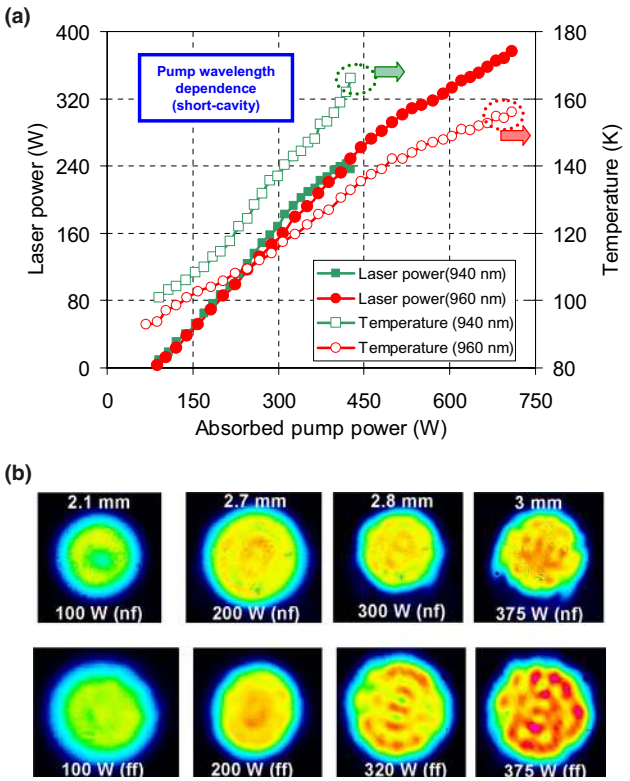


**Fig. 3** **a** Measured variation of cryogenic Yb:YLF cw laser performance with pump wavelength: 940 nm versus 960 nm pumping. Measured variation of average crystal temperature versus absorbed pump power is also shown. The data are taken using the 1%-doped Yb:YLF crystal in the short flat–flat cw cavity using a 25% output coupler. **b** Sample near-field (nf) and far-field (ff) beam profiles of the short-cavity cw Yb:YLF cryogenic laser

It is very elucidating to track the variation of measured crystal temperature as a function of absorbed pump power. As we can see from Fig. 3a, for 960 nm pumping, the average temperature of the crystal increases gradually from 78 to 156 K as the absorbed pump power increases to 700 W (with a slope of around 0.11 K/W: ~ 1.1 K increase in crystal temperature per 10 W of absorbed pump power). Note that assuming a fractional heat load 1.5 times the quantum defect 8.5% [2], the total estimated heat load on the crystal is around 60 W at this absorbed pump power level. This corresponds to a ~ 1.3 K increase in average crystal temperature per 1 W of thermal load. In an earlier numerical study, we have estimated an average temperature of 120 K for a 1% Yb:YLF crystal at 400 W absorbed pump power corresponding to a thermal load of about 33 W or 1.27 K temperature increase per W of thermal load [41]. At 400 W absorbed pump power, we observed a crystal temperature of around 125 K, which demonstrates that the average crystal temperature estimated using the fluorescence intensity ratio method matches the simulation results quite well.

In the experiments, for the 960 nm pumped system, output power scaling of the laser beyond 375 W power level was not possible because of deteriorating output beam quality and lack of cavity stability caused by thermally induced lensing effect. Once the temperature of the crystal reached ~ 155–160 K, the cavity became unstable: the laser was harder to align and the beam profile and laser output were fluctuating. Sample near-field and far-field beam profiles of the laser output are shown in Fig. 3b. As one can see, initially the beam is quite symmetric and homogeneous. As the laser power increases, the laser output slowly becomes super-Gaussian (mimicking the pump beam profile) and at elevated pump powers, hot spots appear in the beam profile, which eventually prevents further power scaling. The beam quality factor ($M^2$) is measured as low as 1.1 at low power levels (100 W). Similar to the case reported in [34], a measurement of the laser beam divergence angle has shown that the beam quality of the laser increases slowly at elevated powers, but still stays below 3 for all cases.

In comparison, for the 940 nm pump diode, the thermal effects limited the output power to 240 W at an absorbed

pump power of 410 W (incident pump power: 715 W, absorption: ~ 57.3%). Note that, within experimental error bars, the slightly shorter pump wavelength did not significantly change the lasing threshold or the slope efficiency (with respect to absorbed pump power). Under 940 nm pumping, the slope efficiency was 73% but the crystal could not handle a pump power above 400 W: the average power started to decrease and could not be improved via cavity realignment. When we look at the estimated average temperature of the crystals, we clearly see that, for 940 nm pumping, the temperature of the crystal rises with a faster slope of around 0.2 K/W. Part of the faster increase of temperature with 940 nm pumping is of course due to higher quantum defect. On top of this, the lower pump absorption at 940 nm also created an issue for this short flat–flat cavity. As an example, at an incident pump power of 715 W, the crystal absorbed only around 410 W of the pump power, and around 65% of the remaining transmitted pump (~ 200 W) is retroreflected back to the dewar by the flat OC. The retroreflected pump beam had a diameter of around 50 mm at the crystal: did not really help with lasing but created a significant additional heat load on the crystal. Usage of a dichroic output coupler with high transmission at the pump wavelength and 25–30% reflectivity at the lasing wavelength could help to resolve this issue in future studies with similar short flat–flat cavities.

As a side note, the zero-phonon line absorption peak of Yb:YLF lies around 971.7 nm and has a FWHM of around 1 nm at 150 K (typical operation temperature of Yb:YLF rods under heavy thermal load) [32]. For the E//a axis, the lasing peak is around 1018 nm, and the corresponding quantum defect is 4.5%. On the other hand, for the 995 nm peak of E//c axis, the quantum defect is only 2.3%. We believe that a ~ 971.7 nm pumped 995 nm cryogenic Yb:YLF laser system has the potential to generate cw output powers above 1 kW from a single rod (the quantum defect is about 2.5 times lower when compared to a 960 nm pumped 1018 nm laser: assuming the crystal could still handle ~ 60 W thermal load, one rod should be able to absorb 1.75 kW of pump power, and generate cw output powers above 1 kW).

## 3.2 Long-cavity cw lasing results

In this subsection, we will present cw lasing results obtained in the long standing-wave cavity configuration (using the cavity in Fig. 1b). To start, Fig. 4 shows cw performance comparison of short and long cavities while using the 960 nm pump source. With the long-cavity, cw laser power up to 325 W was obtained at an absorbed pump power of 717 W (incident power 843 W). The lasing threshold was 60 W (~ 25 W lower than for the short cavity), and the laser slope efficiency with respect to absorbed pump power was around 50% (~ 10% lower compared to the short-cavity). It

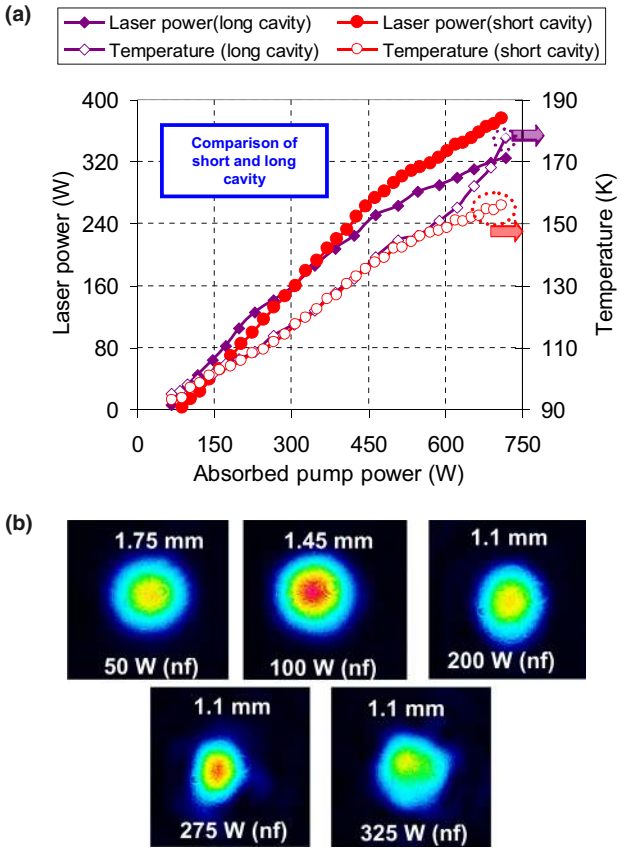


**Fig. 4** **a** Measured variation of cryogenic Yb:YLF cw laser performance with cavity configuration: comparison between the short flat–flat cavity and the long standing-wave cavity (comparison of cavities in Fig. 1a and b). Variation of measured average crystal temperature with absorbed pump power level is also shown for both cases. The data are taken using the 1%-doped Yb:YLF crystal, by employing a pump spot diameter of 2.1 mm with the 960 nm pump. **b** Sample near-field (nf) beam profiles of the long-cavity Yb:YLF cryogenic cw laser

is also instructive to see that, for both short and long cw cavities, the measured average temperature of the crystal increases with a similar trend, except above-absorbed pump powers of 500 W, where the lower performance of the long-cavity laser creates additional heat load. Overall, we can argue that, the long cavity with curved mirrors, provides a cavity mode that enables a lower lasing threshold. On the other hand, it is harder to mode-match to the multimode super-Gaussian pump beam profile, which results in a lower slope efficiency. As a benefit, the beam profile of the laser output is more symmetric/homogeneous, and most of the laser power is contained in the $TEM_{00}$ beam profile (Fig. 4 b). From the measured variation of the near field beam profile (beam profile on the OC mirror), we have estimated a positive thermal lens as strong as + 2 m inside the Yb:YLF gain medium at an absorbed pump power of 700 W. The thermal coefficient of the refractive index for YLF is known

to be negative [31]; hence, contributions from the surface-induced deformations (thermal expansions), population/electronic lensing, and/or photoelastic effect should be the cause of the overall positive thermal lens [42–44].

We have also tested the laser performance using a lower Yb-doped YLF crystal, as it is clear that, the thermal lens originating at elevated temperatures limits the output powers with the 1%-doped crystal. Figure 5 shows the performance of the 2 cm long 0.5% Yb-doped crystal in comparison with the 2 cm long 1% Yb-doped YLF crystal under same conditions. The lasing threshold level with respect to absorbed pump power was similar for both dopings (60 W). Within experimental errors, the slope efficiencies were also similar, but with the 0.5% Yb-doped crystal the obtainable output power was lower. To be more specific, the laser provided 250 W of output power at an absorbed pump power of 520 W (incident power: 915 W, absorption: 56.8%). When we look at the estimated temperature of the crystals, we see that the temperature increase in both crystals is roughly similar, and at 500 W absorbed pump power, the temperature of the 0.5%-doped crystal is about 145 K, which still allows for stronger pumping. We have realized that it is hard to obtain absorbed pump powers above 500 W from the 2 cm long 0.5%-doped YLF crystal for the spot size of 2.2 mm, even under lasing conditions due to: (i) decreasing small-signal absorption with temperature, (ii) limitations of single-pass pumping (limited length and doping), and (iii) onset of pump saturation effect (bleaching of ground-state).

As a closing note, earlier [34, 41] without the knowledge of average crystal temperature, we have attributed the lower performance of the 0.5% crystal to the limited heat extraction capability of the boiling liquid nitrogen boundary (Leidenfrost effect limitation) [45–48]. Recent temperature measurements that we are presenting in this work show that the limited performance of the 0.5%-crystal is most probably due to heating induced pump saturation of the crystal and we are not yet limited by the heat extraction capability of the system.

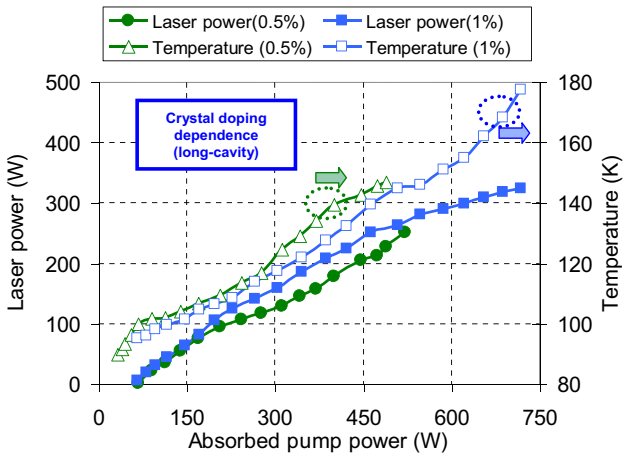


**Fig. 5** Measured variation of cryogenic Yb:YLF cw laser performance with Yb-doping level of the crystal for the long standing-wave laser cavity: 0.5 versus 1% doping. Variation of estimated average crystal temperature with absorbed pump power level is also shown. The data are taken using the long-standing short flat–flat cw cavity, using a pump spot diameter of 2.1 mm with the 960 nm pump

### 3.3 Regenerative amplification results

In this last subsection, we present regenerative amplification results taken with the 1% Yb-doped YLF crystal and discuss the observed limitations. The regenerative amplifier is operated at 10 kHz repetition rate to check the average power scaling potential of the system. Figure 6a shows the obtained pulse energy as a function of absorbed pump power at cavity round-trip numbers 95, 100 and 105. Measured average temperature of the crystal is also shown for the case of 100 round-trips (a similar temperature trend is observed for others). The best regen performance was obtained at 100 regen round trips, where we have reached average regen powers above 90 W (9 mJ at 10 kHz) at an absorbed pump power of 500 W (incident power: 580 W, absorption: 86.2%). At ~ 85 W average output power, we have measured

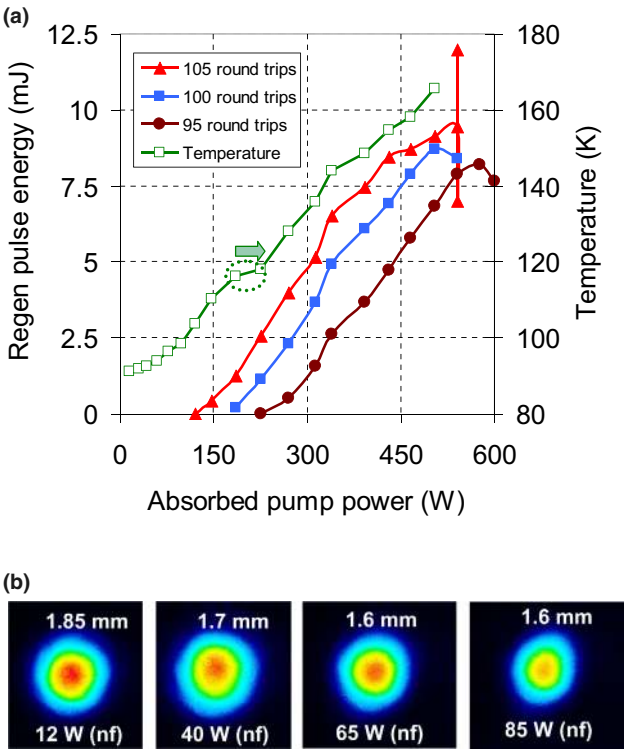


**Fig. 6** **a** Measured performance of cryogenic Yb:YLF regenerative amplifier using the 1% Yb-doped YLF crystal at different round-trip numbers. Variation of measured average crystal temperature with absorbed pump power is also shown. **b** Sample near-field (nf) beam profiles of the regenerative amplifier output

a shot-to-shot rms energy stability below 4% in a 5 min interval (Fig. 7 shows a sample measurement with 3.65% rms noise). During the noise measurements, the amplifier setup was not fully covered, and better performance could potentially be achieved in a well-covered and temperature-stabilized system. Due to the flat gain-profile of E//a axis, the gain narrowing effect was not strong, and the systems preserved bandwidth of the seed pulses (FWHM: ~ 2 nm, typical spectra shown in [36]). At all output power levels, the regenerative amplifier output beam profile was $TEM_{00}$, and the beam quality factor was below 1.2 (Fig. 6b). Further increase of the regenerative cavity output power to around 95 W was possible but resulted in bifurcation behavior of the regen [49, 50]. This bifurcation instability could be suppressed by increasing gain via stronger pumping, but the thermal effects limited this approach in our case: as is also evident from the measured reduction of output beam size (shown in Fig. 6b), the thermally induced lens in the Yb:YLF crystal becomes strong. From the measured variation of the output beam profile, we estimated a thermal lens focusing strength as large as + 2.5 m at an absorbed pump power of 500 W.

In our experiments, we have also realized a considerable amount of depolarization loss in the regenerative amplifier setup (measured via the rejection port of the thin-film polarizers). This motivated us to measure the absorbed pump power dependence of depolarization loss in the 1% Yb:YLF crystal. Figure 8 shows this data along with the measurement of small-signal gain and average crystal temperature. We see that the small-signal gain attainable from the system increases almost linearly with absorbed pump power (only a small decrease of the slope is observed probably due to reduced emission cross section with temperature [32]). As an example, the system reaches a single-pass gain of around 1.6 (60%) at an absorbed pump power of 470 W (2.1 mm pump diameter).

On the other hand, the depolarization loss, which is below 0.5% for the cold crystal, increases to 2.3% level at an absorbed pump power of 470 W. We note here that, it

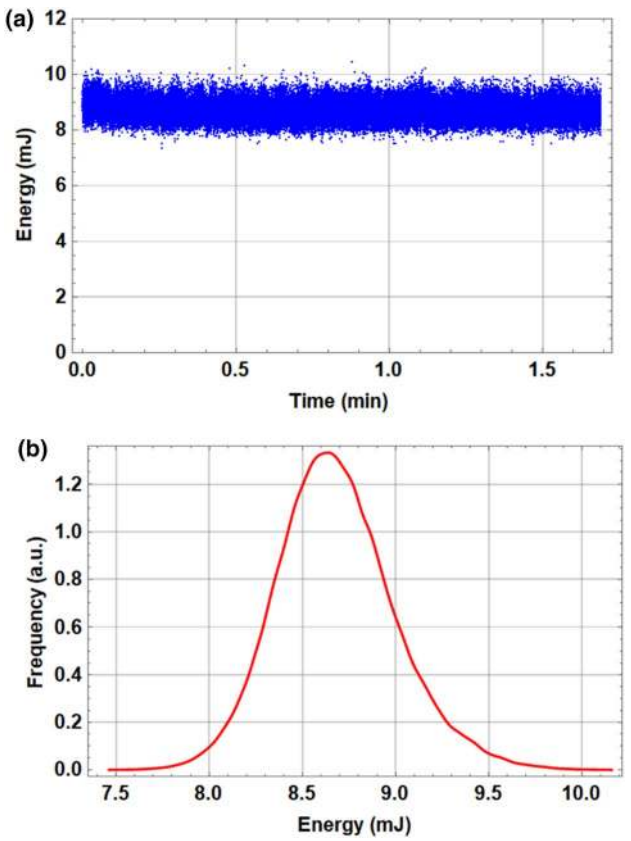


**Fig. 7** **a** Measured variation of Yb:YLF regenerative amplifier energy for a sample 1.7 min time interval (a shot to shot output energy measurement at 10 kHz). **b** Histogram of the regen energy data shown in **a**. Mean regen energy 8.68 mJ, maximum energy: 10.42 mJ, minimum energy:7.34 mJ, standard deviation: 0.32 mJ

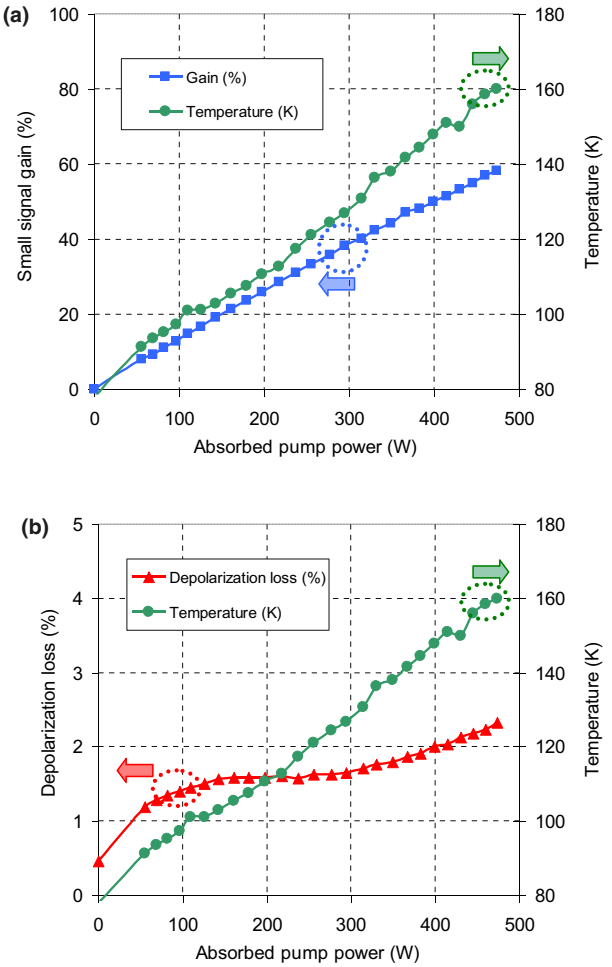


**Fig. 8** Measured variation of small signal gain and depolarization loss with absorbed pump power for the 2 cm long 1% Yb-doped YLF crystal (pump and seed spot diameter: ~ 2.1 mm). Variation of measured average crystal temperature with absorbed pump power level is also shown

was not possible to minimize the depolarization loss further by fine-tuning the tilting of the crystal. We think that the observed depolarization is possibly due to the error margins in the bonding of the undoped and doped YLF parts together, where a few degrees of error in crystal cut direction determination could result in the observed depolarization effect [51]. This clearly shows that ultimate care needs to be taken in minimizing the crystal axis determination errors both in the doped and undoped parts of the YLF crystal. A simple simulation of the system shows that [41], the obtainable average power could easily be scaled to above 125 W when eliminating the depolarization loss observed in this study.

For comparison, regenerative amplification with the 0.5% Yb-doped YLF crystal resulted in 70 W of average power at 10 kHz repetition rate [36]. For the 0.5% doped crystal, the observed depolarization loss was not as high, showing that crystal orientation in the doped and undoped sections matched better for this gain assembly.

## 4 Conclusion

In this study, we have investigated the limitations of the rod geometry in cryogenic Yb:YLF systems. We have experimentally demonstrated the advantages of lower quantum defect pumping for power scaling. Record cw average power approaching 400 W was obtained with the E//a axis, and the thermal lens induced by the transverse temperature gradient in rod geometry is shown to be the main limiting factor for further output power increase. Regenerative amplification at 10 kHz resulted in an average power above 90 W, which can potentially be improved to above 125 W level by minimizing the depolarization losses.

Usage of (i) lower quantum defect pumping via employing the 971.5 nm line, (ii) longer crystals with lower doping (0.5% to 1% Yb-doped 3–4 cm long samples), (iii) E//c axis with the higher gain cross section, (iv) double-crystal geometry [41, 52] and (v) slab and thin-disk geometry are all interesting paths for further improvement to kW level in cw regime and 500 W level in regenerative amplification regime.

**Acknowledgements** The authors acknowledge support from previous group members L. E. Zapata, K. Zapata for establishing the indium-bonding technology for YLF at CFEL-DESY. UD acknowledges support from BAGEP Award of the Bilim Akademisi.

**Funding** Open Access funding enabled and organized by Projekt DEAL. Seventh Framework Programme (FP7) FP7/2007–2013 European Research Council (ERC) (609920).

## Compliance with ethical standards

**Conflict of interest** The authors declare no conflicts of interest.



## References

1. P. Lacovara, H.K. Choi, C.A. Wang, R.L. Aggarwal, T.Y. Fan, Room-temperature diode-pumped Yb:YAG laser. Opt. Lett. **16**, 1089–1091 (1991)
2. T.Y. Fan, Heat Generation in Nd:YAG and Yb:YAG. IEEE J. Quantum Electron. **29**, 1457–1459 (1993)
3. D.C. Brown, T.M. Bruno, J.M. Singley, Heat-fraction-limited CW Yb:YAG cryogenic solid-state laser with 100% photon slope efficiency. Opt. Express **18**, 16573–16579 (2010)
4. L.D. DeLoach, S.A. Payne, L.L. Chase, L.K. Smith, W.L. Kway, W.F. Krupke, Evaluation of absorption and emission properties of Yb doped crystals for laser applications. IEEE J. Quant. Electr. **29**, 1179–1191 (1993)
5. M. Eichhorn, Quasi-three-level solid-state lasers in the near and mid infrared based on trivalent rare earth ions. Appl Phys B-Lasers O **93**, 269–316 (2008)
6. T. Dietz, M. Jenne, D. Bauer, M. Scharun, D. Sutter, A. Killi, Ultrafast thin-disk multi-pass amplifier system providing 1.9 kW of average output power and pulse energies in the 10 mJ range at 1 ps of pulse duration for glass-cleaving applications. Opt. Express **28**, 11415–11423 (2020)
7. P. Russbueldt, T. Mans, J. Weitenberg, H.D. Hoffmann, R. Poprawe, Compact diode-pumped 1.1 kW Yb:YAG Innoslab femtosecond amplifier. Opt. Lett. **35**, 4169–4171 (2010)
8. J. Fischer, A.C. Heinrich, S. Maier, J. Jungwirth, D. Brida, A. Leitenstorfer, 615 fs pulses with 17 mJ energy generated by an Yb:thin-disk amplifier at 3 kHz repetition rate. Opt. Lett. **41**, 246–249 (2016)
9. E. Innerhofer, T. Sudmeyer, F. Brunner, R. Haring, A. Aschwanden, R. Paschotta, C. Honninger, M. Kumkar, U. Keller, 60-W average power in 810-fs pulses from a thin-disk Yb : YAG laser. Opt. Lett. **28**, 367–369 (2003)
10. H. Fattahi, H. Wang, A. Alismail, G. Arisholm, V. Pervak, A.M. Azzeer, F. Krausz, Near-PHz-bandwidth, phase-stable continua generated from a Yb:YAG thin-disk amplifier. Opt. Express **24**, 24337–24346 (2016)
11. S. Manjooran, A. Major, Diode-pumped 45 fs Yb:CALGO laser oscillator with 1.7 MW of peak power. Opt. Lett. **43**, 2324–2327 (2018)
12. E. Caracciolo, M. Kemnitzer, A. Guandalini, F. Pirzio, A. Agnesi, J.A.D. Au, High pulse energy multiwatt Yb:CaAlGdO4

and Yb:CaF2 regenerative amplifiers. Opt. Express **22**, 19912–19918 (2014)
13. A. Diebold, F. Emaury, C. Schriber, M. Golling, C.J. Saraceno, T. Sudmeyer, U. Keller, SESAM mode-locked Yb:CaGdAlO4 thin disk laser with 62 fs pulse generation. Opt. Lett. **38**, 3842–3845 (2013)
14. F. Brunner, T. Sudmeyer, E. Innerhofer, F. Morier-Genoud, R. Paschotta, V.E. Kisel, V.G. Shcherbitsky, N.V. Kuleshov, J. Gao, K. Contag, A. Giesen, U. Keller, 240-fs pulses with 22-W average power from a mode-locked thin-disk Yb : KY(WO4)(2) laser. Opt. Lett. **27**, 1162–1164 (2002)
15. M. Seidel, J. Brons, G. Arisholm, K. Fritsch, V. Pervak, O. Pronin, Efficient high-power ultrashort pulse compression in self-defocusing bulk media. Sci. Rep. **7**, 1–8 (2017)
16. A. Bensalah, Y. Guyot, M. Ito, A. Brenier, H. Sato, T. Fukuda, G. Boulon, Growth of Yb3+-doped YLiF4 laser crystal by the Czochralski method. Attempt of Yb3+ energy level assignment and estimation of the laser potentiality. Opt. Mater. **26**, 375–383 (2004)
17. J.L. Doualan, R. Moncorge, Laser crystals with low phonon frequencies. Ann Chim-Sci Mat **28**, 5–20 (2003)
18. M. Eichhorn, Fluorescence reabsorption and its effects on the local effective excitation lifetime. Appl Phys B-Lasers O **96**, 369–377 (2009)
19. D.C. Brown, S. Tornegard, J. Kolis, C. McMillen, C. Moore, L. Sanjeewa, C. Hancock, The application of cryogenic laser physics to the development of high average power ultra-short pulse lasers. Appl. Sci. **6**, 23 (2016)
20. F. Saltarelli, A. Diebold, I.J. Graumann, C.R. Phillips, U. Keller, Self-phase modulation cancellation in a high-power ultrafast thin-disk laser oscillator. Optica **5**, 1603–1606 (2018)
21. F. Saltarelli, I.J. Graumann, L. Lang, D. Bauer, C.R. Phillips, U. Keller, Power scaling of ultrafast oscillators: 350-W average-power sub-picosecond thin-disk laser. Opt. Express **27**, 31465–31474 (2019)
22. J. Kawanaka, H. Nishioka, N. Inoue, K. Ueda, Tunable continuous-wave Yb : YLF laser operation with a diode-pumped chirped-pulse amplification system. Appl. Opt. **40**, 3542–3546 (2001)
23. D. Alderighi, A. Pirri, G. Toci, M. Vannini, Tunability enhancement of Yb:YLF based laser. Opt. Express **18**, 2236–2241 (2010)
24. F. Pirzio, L. Fregnani, A. Volpi, A. Di Lieto, M. Tonelli, A. Agnesi, 87 fs pulse generation in a diode-pumped semiconductor saturable absorber mirror mode-locked Yb:YLF laser. Appl. Opt. **55**, 4414–4417 (2016)
25. M. Vannini, G. Toci, D. Alderighi, D. Parisi, F. Cornacchia, M. Tonelli, High efficiency room temperature laser emission in heavily doped Yb : YLF. Opt. Express **15**, 7994–8002 (2007)
26. W. Bolanos, F. Starecki, A. Braud, J.L. Doualan, R. Moncorge, P. Camy, 2.8 W end-pumped Yb3+:LiYF4 waveguide laser. Opt. Lett. **38**, 5377–5380 (2013)
27. K. Beil, S. T. Fredrich-Thornton, C. Kränkel, K. Petermann, D. Parisi, M. Tonelli, and G. Huber, "New thin disk laser materials: Yb:ScYLO and Yb:YLF," in *Conference on Lasers and Electro-Optics Europe*(IEEE, Munich, Germany, 2011).
28. J. Kawanaka, S. Tokita, H. Nishioka, M. Fujita, K. Yamakawa, K. Ueda, Y. Izawa, Dramatically improved laser characteristics of diode-pumped Yb-doped materials at low temperature. Laser Phys. **15**, 1306–1312 (2005)
29. J. Kawanaka, K. Yamakawa, H. Nishioka, K. Ueda, Improved high-field laser characteristics of a diode-pumped Yb: LiYF4 crystal at low temperature. Opt. Express **10**, 455–460 (2002)
30. D. Rand, D. Miller, D.J. Ripin, T.Y. Fan, Cryogenic Yb3+-doped materials for pulsed solid-state laser applications [Invited]. Opt. Mater. Express **1**, 434–450 (2011)
31. R. L. Aggarwal, D. J. Ripin, J. R. Ochoa, and T. Y. Fan, "Measurement of thermo-optic properties of Y3Al5O12, Lu3Al5O12, YAIO(3), LiYF4, LiLuF4, BaY2F8, KGd(WO4)(2), and KY(WO4)(2) laser crystals in the 80–300 K temperature range," Journal of Applied Physics **98** (2005).
32. U. Demirbas, J. Thesinga, M. Kellert, F.X. Kärtner, M. Pergament, Detailed investigation of absorption, emission and gain in Yb:YLF in the 78–300 K range. Opt. Mater. Express **11**, 250–272 (2021)
33. L.E. Zapata, D.J. Ripin, T.Y. Fan, Power scaling of cryogenic Yb:LiYF4 lasers. Opt. Lett. **35**, 1854–1856 (2010)
34. U. Demirbas, H. Cankaya, J. Thesinga, F.X. Kärtner, M. Pergament, Efficient, diode-pumped, high-power (>300W) cryogenic Yb:YLF laser with broad-tunability (995–1020.5 nm): investigation of E//a-axis for lasing. Opt. Express **27**, 36562–36579 (2019)
35. D.E. Miller, J.R. Ochoa, T.Y. Fan, Cryogenically cooled, 149 W, Q-switched, Yb:LiYF4 laser. Opt. Lett. **38**, 4260–4261 (2013)
36. U. Demirbas, H. Cankaya, Y. Hua, J. Thesinga, M. Pergament, F.X. Kärtner, 20-mJ, sub-ps pulses at up to 70 W average power from a cryogenic Yb:YLF regenerative amplifier. Opt. Express **28**, 2466–2479 (2020)
37. D.E. Miller, L.E. Zapata, D.J. Ripin, T.Y. Fan, Sub-picosecond pulses at 100 W average power from a Yb:YLF chirped-pulse amplification system. Opt. Lett. **37**, 2700–2702 (2012)
38. U. Demirbas, J. Thesinga, H. Cankaya, M. Kellert, F.X. Kärtner, M. Pergament, High-power passively mode-locked cryogenic Yb:YLF laser. Opt. Lett. **45**, 2050–2053 (2020)
39. Y. Hua, W. Liu, M. Hemmer, L.E. Zapata, G.J. Zhou, D.N. Schimpf, T. Eidam, J. Limpert, A. Tunnermann, F.X. Kartner, G.Q. Chang, 87-W 1018-nm Yb-fiber ultrafast seeding source for cryogenic Yb: yttrium lithium fluoride amplifier. Opt. Lett. **43**, 1686–1689 (2018)
40. U. Demirbas, J. Thesinga, M. Kellert, F.X. Kärtner, M. Pergament, Comparison of different in situ optical temperature probing techniques for cryogenic Yb:YLF. Opt. Mater. Express **10**, 3403–3413 (2020)
41. U. Demirbas, H. Cankaya, J. Thesinga, F.X. Kärtner, M. Pergament, Power and energy scaling of rod-type cryogenic Yb:YLF regenerative amplifiers. J. Opt. Soc. Am B **37**, 1865–1877 (2020)
42. V.V. Zelenogorskii, E.A. Khazanov, Influence of the photoelastic effect on the thermal lens in a YLF crystal. Quantum Electron. **40**, 40–44 (2010)
43. O. Slezak, A. Lucianetti, M. Divoky, M. Sawicka, T. Mocek, Optimization of Wavefront Distortions and Thermal-Stress Induced Birefringence in a Cryogenically-Cooled Multislab Laser Amplifier. IEEE J. Quantum Electron. **49**, 960–966 (2013)
44. Z.L. Zhang, Q. Liu, M.M. Nie, E.C. Ji, M.L. Gong, Experimental and theoretical study of the weak and asymmetrical thermal lens effect of Nd:YLF crystal for sigma and pi polarizations. Appl Phys B-Lasers O **120**, 689–696 (2015)
45. M. Kida, Y. Kikuchi, O. Takahashi, I. Michiyoshi, Pool-Boiling Heat-Transfer in Liquid-Nitrogen. J. Nucl. Sci. Technol. **18**, 501–513 (1981)
46. K. Bouazaoui, R. Agounoun, K. Sbai, A. Zoubir, I. Kadiri, M. Rahmoune, R. Saadani, Experimental and numerical study of pool boiling heat transfer of liquid nitrogen LN2: application to the brass ribbon cooling in horizontal position. Int. J. Mech. Mechatron. Eng. **17**, 74–82 (2017)
47. H. Hu, C. Xu, Y. Zhao, K. J. Ziegler, and J. N. Chung, "Boiling and quenching heat transfer advancement by nanoscale surface modification," Scientific Reports **7** (2017).
48. C. Kruse, T. Anderson, C. Wilson, C. Zuhlke, D. Alexander, G. Gogos, S. Ndao, Extraordinary shifts of the Leidenfrost

temperature from multiscale micro/nanostructured surfaces. Langmuir **29**, 9798–9806 (2013)
49. P. Kroetz, A. Ruehl, A.L. Calendron, G. Chatterjee, H. Cankaya, K. Murari, F.X. Kartner, I. Hartl, R.J.D. Miller, Study on laser characteristics of Ho: YLF regenerative amplifiers: operation regimes, gain dynamics, and highly stable operation points. Appl Phys B-Lasers O. **123**, 126 (2017)
50. J. Dörring, A. Killi, U. Morgner, A. Lang, M. Lederer, D. Kopf, Period doubling and deterministic chaos in continuously pumped regenerative amplifiers. Opt Express **12**, 1759–1768 (2004)
51. P.D. Hale, G.W. Day, Stability of Birefringent linear retarders (Waveplates). Appl. Opt. **27**, 5146–5153 (1988)
52. E.C. Honea, R.J. Beach, S.C. Mitchell, J.A. Skidmore, M.A. Emanuel, S.B. Sutton, S.A. Payne, P.V. Avizonis, R.S. Monroe, D.G. Harris, High-power dual-rod Yb : YAG laser. Opt. Lett. **25**, 805–807 (2000)